The Imine-Based COF TpPa-1 as an Efficient Cooling Adsorbent That Can Be Regenerated by Heat or Light

Javier Pérez-Carvajal, Gerard Boix, Inhar Imaz,* and Daniel Maspoch*

Javier Pérez-Carvajal, Gerard Boix, Inhar Imaz, and Daniel Maspoch:
Catalan Institute of Nanoscience and Nanotechnology (ICN2)CSIC and BIST
Campus UAB, Bellaterra08193 Barcelona, Spain
E-mail: inhar.imaz@icn2.cat; daniel.maspoch@icn2.cat
Prof. D. Maspoch:
ICREA
Pg. Lluís Companys 23, Barcelona 08010, Spain

Adsorption-based cooling systems, which can be driven by waste heat and solar energy, are promising alternatives to conventional, compression-based cooling systems, as they demand less energy and emit less CO_2. The performance of adsorption-based cooling systems relates directly to the performance of the working pairs (sorbent–water). Accordingly, improvement of these systems relies on the continual discovery of new sorbents that enable greater mass exchange while requiring less energy for regeneration. Here, it is proposed that covalent-organic frameworks (COFs) can replace traditional sorbents for adsorption-based cooling. In tests mimicking standard operating conditions for industry, the imine-based COF TpPa-1 exhibits a regeneration temperature below 65 °C and a cooling coefficient of performance of 0.77 – values which are comparable to those reported for the best metal–organic framework sorbents described to date. Moreover, TpPa-1 exhibits a photothermal effect and can be regenerated by visible light, thereby opening the possibility for its use in solar-driven cooling.

Increasing fuel consumption and prices, combined with anthropogenic greenhouse gas emissions, are together driving the development of new technologies and materials to reduce society's electrical energy demands. Already, more than 44% of all primary energy in the US residential and commercial sectors is consumed by environmental control systems such as cooling devices, and this percentage is predicted to increase (**https://www.iea.org/weo2017/**). To reverse such consumption, several initiatives have been proposed, including use of adsorption heat transformation and storage (AHTS) systems, such as adsorption-cooling systems/chillers, heat pumps, and thermal batteries.[1-3] These systems employ energy-delivery processes based on a reversible adsorption/desorption cycle of a working fluid, whereby useful heat is released during the exothermal adsorption step and cold is produced during the evaporation of the fluid. Among their advantages, these systems enable use of low thermal-energy sources (e.g., solar radiation and waste heat) for regeneration and driving energy, and use of water as the working fluid.[4] The efficiency of these processes relates directly to the performance of the working pairs (adsorbent–adsorbate) in terms of both the level of mass exchange and the amount of heat required for regeneration.[5] Commercially[6] available, thermally driven adsorption chillers and heat pumps employ traditional porous sorbents such as silica, activated carbon, and zeolites. However, these porous materials have limited performance, exhibiting very low adsorption uptake in the working range (0.05–0.32% relative humidity) and requiring high temperatures for regeneration.[7-10]

Metal–organic frameworks (MOFs) are an emerging class of versatile porous materials that have recently been proposed for AHTS applications,[11-14] as they can take up large amounts of water within the abovementioned working range and show “S-”type sorption isotherms (e.g., type IV/V). Such isotherms are desirable for AHTS applications since their maximum working capacity falls within a very narrow window of relative pressure (or relative humidity). Under these conditions, porous materials can be easily regenerated upon small variations in temperature and can reversibly adsorb/desorb

water upon minor changes in relative water pressure (or relative humidity). For cooling applications, this steep increase should ideally occur between $0.05 < P/P_0 < 0.32$[7] and the regeneration temperature should be close to that of the cogeneration plants for building heating (≈65 °C).[14] To date, the most promising water-stable MOFs displaying S-shape isotherms in the chilling range are MIL-125-NH_2,[12] Al-fum,[15] Zr-fum,[16] CAU-10,[17] MIP-200,[14] and Co_2Cl_2(BTDD).[18] Table 1 summarizes values of some performance parameters for these MOFs when used as cooling adsorbents.

- Insert Table 1 –

A principal concern with use of MOFs in water-based applications is their long-term stability, suggesting the need for alternative porous materials.[19] An interesting candidate is covalent-organic frameworks (COFs),[20, 21] which have recently been proposed for water-based applications, as they exhibit high water uptake and S-shape isotherms in the range of interest (0.05–0.32 P/P_0),[22] while also showing high structural and chemical tunability and remaining relatively chemically stable to water, to acid, and under redox conditions.[23-28] A particularly promising COF for water-based applications is TpPa-1.[29] First reported by Banerjee and co-workers in 2012,[30] TpPa-1 is a 2D imine-based COF that comprises 1,3,5-triformylphloroglucinol (Tp) and *p*-phenylenediamine (Pa-1) (Figure 1a), exhibits a water uptake of 30 wt% at 0.3 P/P_0,[29] is highly stable in water, and is bulk-scale processable.[31] Accordingly, it was described to be an excellent desiccant under ambient conditions.

-Insert figure 1-

Herein, we report that TpPa-1 can serve as an efficient adsorbent for cooling systems in cogeneration plants that typically work around 65 °C. We show that TpPa-1 can operate at a regeneration temperature below 65 °C (temperature needed for complete water desorption). In tests mimicking standard operating conditions for industry, its cooling coefficient of performance (COP_C) was 0.77. Finally, we demonstrate that visible light can be used to regenerate TpPa-1 (i.e., remove all its water molecules) and consequently, to drive the cooling process.

TpPa-1 was synthesized following the procedure of Banerjee and co-workers.[29] A mixture of Tp and Pa-1 (1:1.5 molar ratio) was dissolved in a mixture of 1,4-dioxane and mesitylene, and the resulting solution was mixed with acetic acid. Then, this solution was heated at 120 °C for 3 days in a sealed glass reactor, ultimately yielding a bright red solid, which was gently washed with *N*,*N*-dimethylacetamide, acetone, and tetrahydrofuran. X-ray powder diffraction (XRPD) of the resultant powder after overnight drying (dynamic vacuum; 80 °C) indicated formation of the expected eclipsed crystalline phase of TpPa-1 (Figure 1b). Nitrogen physical-adsorption measurements on a sample of TpPa-1 outgassed at 120 °C followed a pure type I isotherm,[32] and the calculated Brunauer–Emmett–Teller (BET) surface area was 840 $m^2\,g^{-1}$ (Figure S1, Supporting Information).[29] The pore volume was also accessible to CO_2, with a total amount of 11.1 mmol g^{-1} at 760 Torr (Figure S2, Supporting Information). The collected water isotherm revealed an "S-"type sorption isotherm, exhibiting a main, steep uptake at α = 0.22 and a maximum uptake of 0.45 $g_{water}\,g_{COF}^{-1}$ at 0.90 P/P_0 (Figure 1c). This S-shape trend is associated with an initial sorption of water molecules around the polar groups of the framework via hydrogen bonding, which leads to gradual formation of a monolayer on the inner surface of the pore before the hole cavity becomes filled.[33] Importantly, all these sorption data are fully consistent with previously reported values for this COF.[29]

The energy efficiency of porous materials for cooling applications is commonly determined by their COP_C,[7] which is defined as the ratio of vaporization heat (Q_{ev}) to regeneration heat (Q_{reg}); in other words: the useful output energy obtained in function of the energy demand (Equations (S1)–(S5) and Figure S3, Supporting Information). To evaluate both Q_{ev} and Q_{reg}, we analyzed an isosteric cycle

diagram of an adsorption air-conditioning cycle to determine the working capacity (Δw) of the working pair TpPa-1/H_2O and the desorption temperature (T_{des}) (Figure 2a). This diagram was calculated using the water adsorption isobars in a range of water-vapor pressure values (0.7, 1.2, 2.4, 3.7, and 5.6 kPa) and under variable T_{des} (Figure S4, Supporting Information), with the operational temperature of the cycle evaporation (T_{ev}) fixed at 10 °C, and the temperature of adsorption and condensation ($T_{ad} = T_{con}$), at 30 °C. During isobaric adsorption (step IV–I), TpPa-1 adsorbed water, reaching a maximum uptake of 0.27 $g_{water}\ g_{COF}^{-1}$. Then, during isosteric heating (I–II), TpPa-1 became fully saturated and the pressure increased from 1.2 to 4.2 kPa by increasing the temperature from 30 to 37.2 °C without desorption. During isobaric desorption (II–III), heating continued and desorption proceeded until a T_{des} of 65 °C was reached, at which point the water uptake was minimal. Finally, during isosteric cooling, decreasing the temperature, the pressure was reduced and TpPa-1 was regenerated. Thus, the working capacity depends on T_{des} and increases up to 0.27 $g_{water}\ g_{COF}^{-1}$ at T_{des} = 65 °C or higher.

-insert figure 2-

Next, we determined the heat of adsorption ($\Delta_{ads}H$), by using water isotherms collected at two temperatures (25 and 40 °C; Figure 1c and Figure S5 (Supporting Information)) and by adjusting the obtained values to the Clausius–Clapeyron equation (Equation (S6), Supporting Information). After a high-energy interaction at low coverage (70 kJ mol^{-1}), the $\Delta_{ads}H$ decayed down to 45–50 kJ mol^{-1}, showing a value closer to that of the enthalpy of evaporation of water (Figure 1d).[34] This low value was attributed to water–water molecular interactions, which are more favorable than COF–water interactions. Note that our determined $\Delta_{ads}H$ as a function of the water uptake closely agrees with a previously reported value from a simulation.[33]

Having determined Δw, T_{des}, and $\Delta_{ads}H$ for TpPa-1, we then calculated its COP_C as a function of T_{des} (Figure 2b). A value of 0.77 was found in the range from 45 to 65 °C. Remarkably, this value falls within the range of reported values for the three highest-performing MOFs (MIP-200, Co_2Cl_2[BTDD], and CAU-10), which can perform at full efficiency in building–heating cogeneration plants (63 °C). Note that we also performed 40 consecutive water adsorption and desorption cycles under near-operational conditions for air-conditioning systems (P = 2.36 kPa, T_{ads} = 303 K, and T_{des} = 383 K; Figure S6, Supporting Information). This cycling experiment corroborated that TpPa-1 exhibits a high degree of stability (Figure S7, Supporting Information), with less than 0.02 $g_{water}\ g_{COF}^{-1}$ loss of uptake after cycling.

Solar collectors are a green alternative to provide the heat required for operation of AHTS systems. For example, they are commonly in demand for nonelectric, water-based refrigerators used for long-term storage of harvested grains; especially for grain silos located in areas with limited access to electricity. Inspired by this precedent and by the photothermal effect that COF exhibits during irradiation (Figure S8, Supporting Information),[35] we explored the use of TpPa-1 as an adsorbent for photoactivated desorption of water (i.e., photoactivated cooling). To this end, TpPa-1 was exposed to visible light at an irradiance of 0.32 mW cm^{-2}. Under these conditions, TpPa-1 immediately heated up, reaching 65 °C in less than 1 min (Figure 3a,c). Once we confirmed that the working desorption temperature could be reached by light irradiation, we then studied the light-triggered release of water in TpPa-1 by coupling the radiation source to the sorption instrument (Figure 3b). At an operating water pressure of 2.36 kPa, TpPa-1 initially adsorbed 0.25 $g_{water}\ g_{COF}^{-1}$. Once the light had been switched on, the water was fully desorbed from TpPa-1. Finally, the on/off light-switching cycle was repeated to perform 15 consecutive adsorption–desorption cycles (Figure 3d), in which no loss of performance was detected. These findings together demonstrated that TpPa-1 could be efficiently regenerated by using visible light.

-insert figure 3-

In conclusion, and to the best of our knowledge, we have reported the first-ever use of a COF (TpPa-1) as an adsorbent in adsorption-based cooling processes. Relative to other MOF-, zeolite-, and silica-based adsorbents previously reported for this application, TpPa-1 exhibits comparable working capacity, a lower energy of adsorption, and a lower regeneration temperature (Table 1).[12, 14-16, 18, 36-42] Accordingly, TpPa-1 ranks alongside the highest-performing MOFs tested to date, showing its full efficiency below 65 °C. Furthermore, we have exploited the photothermal effect of TpPa-1 in the visible region to enable light-triggered water desorption, thus paving the way to use of TpPa-1 in solar-driven cooling. We are confident that the possibility of synthesizing COFs with other chemically stable linkages, such as amine, amide, alkene, and polyarylether,[43, 44] could pave the way to new functional adsorbents for this promising technology to reduce society's electrical energy demands.

Experimental Section

Synthesis of TpPa-1: Tp (0.3 mmol; 63 mg) and Pa-1 (0.45 mmol; 49 mg) were separately dissolved in a 1:1 mixture of mesitylene and 1,4-dioxane (1.5 mL each) and mixed together with 0.5 mL of 8 M acetic acid inside a Pyrex vial (13 mL). The mixture was sonicated for 5 min to assure complete homogenization and then, was heated at 120 °C for 3 days. The resultant bright red solid was filtered off and washed twice with *N*,*N*-dimethylacetamide (10 mL), twice with acetone (10 mL), and once with tetrahydrofuran. The resultant powder was dried under dynamic vacuum at 80 °C overnight.

Methods: XRPD patterns were collected on an X'Pert PRO MPDP analytical diffractometer (Panalytical) at 45 kV, 40 mA using Cu Kα radiation (λ = 1.5419 Å). Volumetric N_2 adsorption–desorption isotherm was collected at 77 K using an ASAP2020 HD (Micromeritics). BET surface area was determined using Microactive software (Micromeritics). Volumetric CO_2 adsorption–desorption isotherm was collected at 203 K using an ASAP2020 HD (Micromeritics) coupled with a chiller. Gravimetric water vapor adsorption–desorption isotherms were measured using a dynamic vapor sorption (DVS) vacuum instrument (Surface Measurement Systems Ltd.). The weight of the dried powder (≈20 mg) was constantly monitored with a high-resolution microbalance (±0.1 μg) and recorded at 25 and 40 °C (±0.2 °C) under pure water-vapor pressures. The kinetics curves of water-vapor adsorption were obtained measuring real-time mass change. The isobars were recorded at different temperatures (range: 110–30 °C) at the fixed pressures of 0.7, 1.2, 2.4, 3.7, and 5.6 kPa. Prior to the sorption experiments, samples were degassed inside the chamber under vacuum at 120 °C for 6 h. The heat-capacity measurements were performed on a differential scanning calorimeter (Mettler Toledo). The heating rate used was 10 °C min^{-1} (range: 10–90 °C) and sapphire was used as a reference material. Visible irradiation was supplied by a Bluepoint 4 Ecocure (Hönle UV Technology) intensity spot lamp (300–650 nm) after a UV filter (300–400 nm). Temperature was recorded in infrared camera PI 450 (Optris), working in the range of 0–250 °C. Data were obtained using the PI Connect software. Light-triggered kinetic water vapor adsorption curves were collected measuring real-time mass change under constant pressure of pure water and by switching the lamp on and off for irradiation cycling. For this application, a DVS vacuum instrument was used as follows (see Figure 3b): by including a glass viewport below the chamber to enable passage of visible light; by using a flat quartz pan; and by aligning the lamp and the pan with a center plug. Solid-state diffusive refraction spectra of the pure powder were recorded using a Cary 4000 spectrophotometer (Agilent Technologies) in the wavelength range of 300–900 nm.

Acknowledgements

This work was supported by the Spanish MINECO (project PN MAT2015-65354-C2-1-R); the Catalan AGAUR (project 2017 SGR 328); the ERC, under EU-FP7 (ERC-Co 615954); and the CERCA Program/Generalitat de Catalunya. ICN2 was supported by the Severo Ochoa program from Spanish MINECO (Grant No. SEV-2017-0706).

Conflict of Interest

The authors declare no conflict of interest.

Keywords

adsorption heat transformation, cooling, covalent-organic framework,

porous materials, visible light

Received: May 10, 2019

Revised: August 7, 2019

Published online: September 3, 2019

References

[1] H. Kummer, F. Jeremias, A. Warlo, G. Fuldner, D. Frohlich, C. Janiak, R. Glaser, S. K. Henninger, *Ind. Eng. Chem. Res.* 2017, *56*, 8393.

[2] S. Narayanan, X. Li, S. Yang, H. Kim, A. Umans, I. S. McKay, E. N. Wang, *Appl. Energy* 2015, *149*, 104.

[3] J. Canivet, A. Fateeva, Y. Guo, B. Coasne, D. Farrusseng, *Chem. Soc. Rev.* 2014, *43*, 5594.

[4] S. K. Henninger, F. P. Schmidt, H. M. Henning, *Adsorption* 2011, *17*, 833.

[5] L. G. Gordeeva, Y. I. Aristov, *Energy* 2019, *167*, 440.

[6] I. S. Girnik, *Energy* 2016, *106*, 13.

[7] M. F. de Lange, K. J. F. M. Verouden, T. J. H. Vlugt, J. Gascon, F. Kapteijn, *Chem. Rev.* 2015, *115*, 12205.

[8] W. Wang, L. Wu, Z. Li, Y. Fang, J. Ding, J. Xiao, *Drying Technol.* 2013, *31*, 1334.

[9] X. Wei, W. Wang, J. Xiao, L. Zhang, H. Chen, J. Ding, *Chem. Eng. J.* 2013, *228*, 1133.

[10] P. Goyal, P. Baredar, A. Mittal, A. R. Siddiqui, *Renewable Sustainable Energy Rev.* 2016, *53*, 1389.

[11] J. Canivet, J. Bonnefoy, C. Daniel, A. Legrand, B. Coasne, D. Farrusseng, *New J. Chem.* 2014, *38*, 3102.

[12] L. G. Gordeeva, M. V. Solovyeva, Y. I. Aristov, *Energy* 2016, *100*, 18.

[13] F. Jeremias, D. Frohlich, C. Janiak, S. K. Henninger, *New J. Chem.* 2014, *38*, 1846.

[14] S. Wang, J. S. Lee, M. Wahiduzzaman, J. Park, M. Muschi, C. Martineau-Corcos, A. Tissot, K. H. Cho, J. Marrot, W. Shepard, G. Maurin, J.-S. Chang, C. Serre, *Nat. Energy* 2018, *3*, 985.

[15] F. Jeremias, D. Frohlich, C. Janiak, S. K. Henninger, *RSC Adv.* 2014, *4*, 24073.

[16] M. V. Solovyeva, L. G. Gordeeva, T. A. Krieger, Y. I. Aristov, *Energy Convers. Manage.* 2018, *174*, 356.

[17] D. Frohlich, E. Pantatosaki, P. D. Kolokathis, K. Markey, H. Reinsch, M. Baumgartner, M. A. van der Veen, D. E. De Vos, N. Stock, G. K. Papadopoulos, S. K. Henninger, C. Janiak, *J. Mater. Chem. A* 2016, *4*, 11859.

[18] A. J. Rieth, S. Yang, E. N. Wang, M. Dincaˇ, *ACS Cent. Sci.* 2017, *3*, 668.

[19] N. C. Burtch, H. Jasuja, K. S. Walton, *Chem. Rev.* 2014, *114*, 10575.

[20] A. P. Cote, A. I. Benin, N. W. Ockwig, M. O'Keeffe, A. J. Matzger, O. M. Yaghi, *Science* 2005, *310*, 1166.

[21] Rebecca L. Li, N. C. Flanders, A. M. Evans, W. Ji, I. Castano, L. X. Chen, N. C. Gianneschi, W. R. Dichtel, *Chem. Sci.* 2019, *10*, 3796.

[22] L. Stegbauer, M. W. Hahn, A. Jentys, G. Savasci, C. Ochsenfeld, J. A. Lercher, B. V. Lotsch, *Chem. Mater.* 2015, *27*, 7874.

[23] N. Huang, P. Wang, D. Jiang, *Nat. Rev. Mater.* 2016, *1*, 16068.

[24] X. Li, C. Zhang, S. Cai, X. Lei, V. Altoe, F. Hong, J. J. Urban, J. Ciston, E. M. Chan, Y. Liu, *Nat. Commun.* 2018, *9*, 2998.

[25] T. Sick, A. G. Hufnagel, J. Kampmann, I. Kondofersky, M. Calik, J. M. Rotter, A. Evans, M. Doblinger, S. Herbert, K. Peters, D. Bohm,

P. Knochel, D. D. Medina, D. Fattakhova-Rohlfing, T. Bein, *J. Am. Chem. Soc.* 2018, *140*, 2085.

[26] P. Pachfule, A. Acharjya, J. Roeser, T. Langenhahn, M. Schwarze, R. Schomacker, A. Thomas, J. Schmidt, *J. Am. Chem. Soc.* 2018, *140*, 1423.

[27] L. Stegbauer, K. Schwinghammer, B. V. Lotsch, *Chem. Sci.* 2014, *5*, 2789.

[28] J. Xie, S. A. Shevlin, Q. Ruan, S. J. A. Moniz, Y. Liu, X. Liu, Y. Li, C. C. Lau, Z. X. Guo, J. Tang, *Energy Environ. Sci.* 2018, *11*, 1617.

[29] B. P. Biswal, S. Kandambeth, S. Chandra, D. B. Shinde, S. Bera, S. Karak, B. Garai, U. K. Kharul, R. Banerjee, *J. Mater. Chem. A* 2015, *3*, 23664.

[30] S. Kandambeth, A. Mallick, B. Lukose, M. V. Mane, T. Heine, R. Banerjee, *J. Am. Chem. Soc.* 2012, *134*, 19524.

[31] S. Karak, S. Kandambeth, B. P. Biswal, H. S. Sasmal, S. Kumar, P. Pachfule, R. Banerjee, *J. Am. Chem. Soc.* 2017, *139*, 1856.

[32] K. S. W. Sing, D. H. Everett, R. A. W. Haul, L. Moscou, R. A. Pierotti, J. Rouquerol, T. Siemienewska, *Pure Appl. Chem.* 1985, *57*, 603.

[33] Y. Ge, H. Zhou, Y. Ji, L. Ding, Y. Cheng, R. Wang, S. Yang, Y. Liu, X. Wu, Y. Li, *J. Phys. Chem. C* 2018, *122*, 27495.

[34] L. Garzon-Tovar, J. Perez-Carvajal, I. Imaz, D. Maspoch, *Adv. Funct. Mater.* 2017, *27*, 1606424.

[35] J. Espin, L. Garzon-Tovar, A. Carne-Sanchez, I. Imaz, D. Maspoch, *ACS Appl. Mater. Interfaces* 2018, *10*, 9555.

[36] B. Shi, R. Al-Dadah, S. Mahmoud, A. Elsayed, *Appl. Therm. Eng.* 2016, *106*, 325.

[37] D. C. Wang, Z. Z. Xia, J. Y. Wu, R. Z. Wang, H. Zhai, W. D. Dou, *Int. J. Refrig.* 2005, *28*, 1073.

[38] C. Y. Tso, C. Y. H. Chao, *Int. J. Refrig.* 2012, *35*, 1626.

[39] L. Z. Zhang, *Appl. Therm. Eng.* 2000, *20*, 103.

[40] F. B. Cortes, F. Chejne, F. Carrasco-Marin, C. Moreno-Castilla, A. F. Perez-Cadenas, *Adsorption* 2010, *16*, 141.

[41] S. Vasta, A. Freni, A. Sapienza, F. Costa, G. Restuccia, *Int. J. Refrig.* 2012, *35*, 701.

[42] M. Fischer, *Phys. Chem. Chem. Phys.* 2015, *17*, 25260.

[43] S. J. Lyle, P. J. Waller, O. M. Yaghi, *Trends Chem.* 2019, *1*, 172.

[44] X. Guan, H. Li, Y. Ma, M. Xue, Q. Fang, Y. Yan, V. Valtchev, S. Qiu, *Nat. Chem.* 2019, *11*, 587.

Adsorbent	H_2O loading [g g^{-1}] at 0.3 P/P_0	T_{des} [°C]	COP_C	$\Delta_{ads}H$ [kJ mol^{-1}]	Refs.
NH_2-MIL-125	0.42	90	0.8	49.7	[12]
CPO-27(Ni)	0.45	130	0.45	62	[36]
Al-fum	0.33	65	–	50	[15]
Zr-fum	0.26	85	0.67	55	[16]
CAU-10	0.30	65	0.73	52	[14]
MIP-200	0.39	65	0.78	45	[14]
Co_2Cl_2(BTDD)	0.86	45	0.90	45.8	[18]
Silica gel	–	85	0.38	–	[37]
Activated carbon	0.19	115	0.37	51.9	[38]
Zeolite 13-X	0.24	310	0.38	61.2	[39,40]
AQSOA-FAM-Z02 (ALPO-34)	0.29	90	0.25–0.3	63.5	[14,41,42]
TpPa-1	0.27	65	0.77	45	This work

Table 1. Comparison of adsorption performance parameters for highperforming MOFs (literature values) and **TpPa-1** (experimental values from this study): water loading, regeneration temperature (*T*des), COPC, and heat of adsorption (Δads*H*).

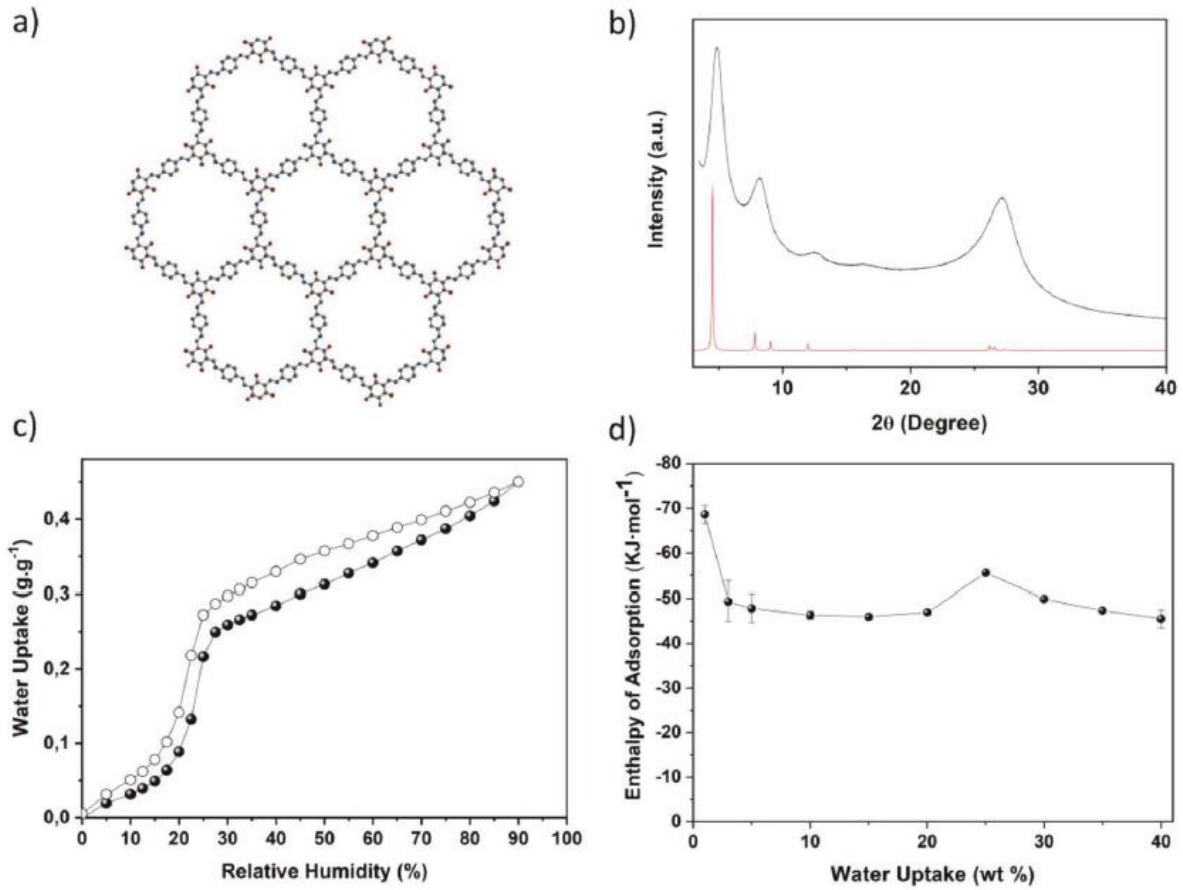

Figure 1. a) The chemical structure of **TpPa-1** (color code: C, gray; N, blue; O, red; H atoms have been omitted for clarity). b) XRPD on the simulated structure (red) and on the experimental data record (black). c) Water adsorption–desorption isotherm at 25 °C. d) Heat of adsorption as a function of loading. Solid dots: adsorption branches; hollow dots: desorption branches.

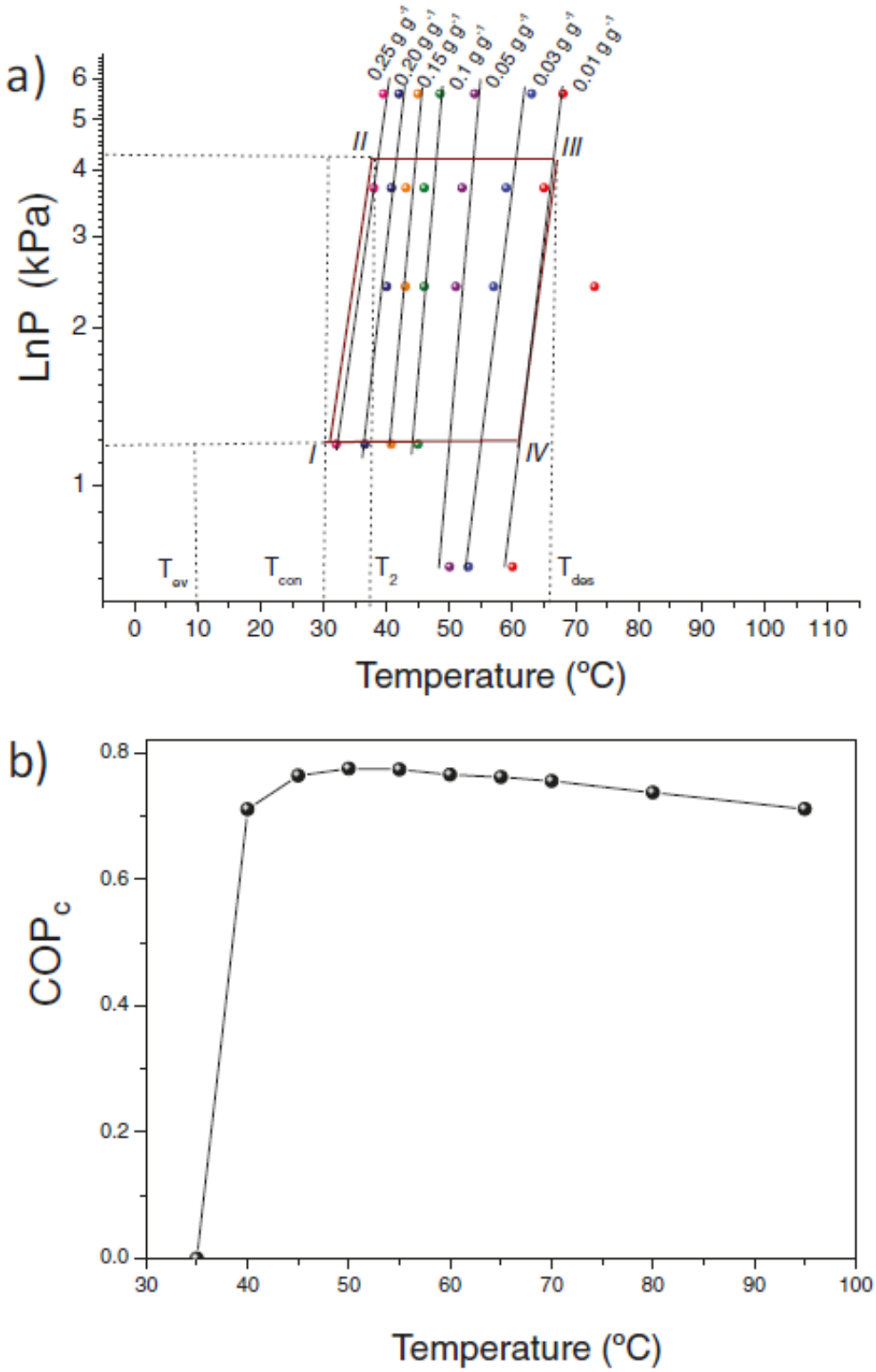

Figure 2. a) Isosteric cycle diagram for the working pair **TpPa-1**/water, calculated for an air-cooling cycle. b) COPC as a function of *T*des for the working pair **TpPa-1**/water.

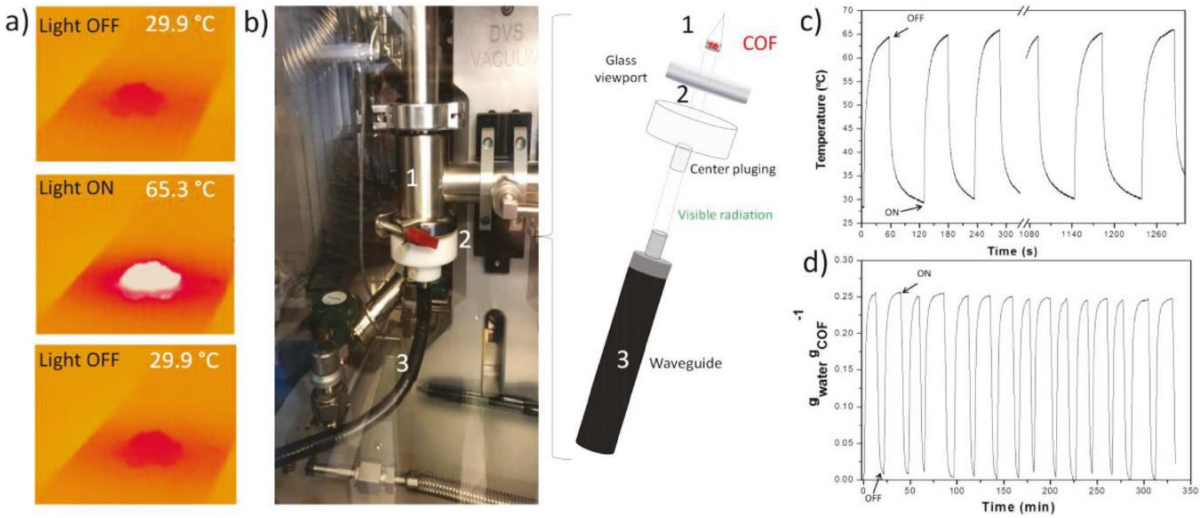

Figure 3. a) IR camera images of **TpPa-1** (top); after 60 s of light irradiation (middle); and after ≈60 s after the light had been switched off (bottom). b) Photograph, and the corresponding scheme of the light coupled to the sorption instrument. c) Temperature cycles induced by switching the light on and off. d) Water adsorption–desorption cycles induced by switching the light on and off.